PHYSICAL REVIEW B VOLUME 23, NUMBER 4 15 FEBRUARY 1981

Electronic structure of metal hydrides. IV. TiH_x, ZrH_x, HfH_x, and the fcc-fct lattice distortion

J. H. Weaver and D. J. Peterman
Synchrotron Radiation Center, University of Wisconsin-Madison, Stoughton, Wisconsin 53589

D. T. Peterson
Ames Laboratory, U.S. Department of Energy, and Department of Materials Science and Engineering, Iowa State University, Ames, Iowa 50011

A. Franciosi
Synchrotron Radiation Center, University of Wisconsin-Madison, Stoughton, Wisconsin 53589 and Istituto di Fisica, Universita di Roma, Rome, Italy

(Received 9 September 1980)

The electronic structures of TiH_x, ZrH_x, and HfH_x have been studied using photoelectron spectroscopy and synchrotron radiation. Structures in the metal d-derived band within ~ 3 eV of the Fermi level E_F and in the bonding band (~ 3–10 eV below E_F) are compared with theory. In each dihydride, the bonding band center falls at -5.5 eV, at approximately the same energy as previously observed for the dihydrides of Sc and Y. Changes in the emission features near E_F and at -7 eV have been observed in samples bridging the fcc→fct distortion in ZrH_x, $1.63 \leq x \leq 1.94$. The changes at E_F demonstrate the Jahn-Teller effect for the electronic states of ZrH_x. The binding energies of the Ti $3p$, Zr $4p$, Hf $5p$, and Hf $4f$ cores are observed to be greater than in the elemental metals, consistent with charge transfer to the hydrogen site.

INTRODUCTION

Many, but not all, transition metals react with hydrogen to form stable metal dihydrides.[1] These interstitial alloys exhibit properties which are quite different from those of the elemental metals, including crystal structures (generally hcp→fcc) and mechanical properties (ductile→brittle). The electronic properties of dihydrides are strikingly different from those of the parent metal, and in a series of recent papers[2–8] we have examined many of the hydrogen-induced band-structure changes. We have shown, for example, that dihydrides exhibit wide metal-hydrogen bonding bands centered about 5.5 eV below the Fermi level E_F, which have no counterpart in the metal band structure, and that the states near E_F are primarily metal d-derived.

The group IIIB metals (Sc, Y, and most lanthanides) and the IVB metals (Ti, Zr, Hf) form stable metallic dihydrides with a CaF_2 crystal structure over a wide range of composition x, where $x = H/M$. In general, the hydrogen atoms occupy the tetrahedral lattice sites. It has recently been observed,[2,9–12] however, that the group IIIB dihydrides can have partial octahedral site occupation for $x \rightarrow 2$. In contrast to this, the group IVB dihydrides exhibit a crystal-structure distortion[1,13,14] from fcc to fct for $x \rightarrow 2$. These deviations from the ideal CaF_2 structure with completely occupied tetrahedral sites suggest that the ideal dihydride is energetically unstable.

We have conducted a series of photoemission experiments to examine the electronic structure of the dihydrides TiH_x, ZrH_x, and HfH_x. Two aspects were particularly interesting. First, we wished to compare the bonding-band energies of the group IVB dihydrides with those of the group IIIB dihydrides to see if the hydrogen-induced bands remained ~ 5.5 eV below E_F as E_F moved higher in the d bands (they did). Second, we wished to observe changes which might accompany the fcc-fct distortion of ZrH_x for $1.63 \leq x \leq 1.94$. We have observed significant changes in the states near E_F and in the deeper-lying states near -7 eV.

This study of the group IVB dihydrides reflects our ongoing interest in the fundamental properties of metal-hydrogen systems. In the first three papers of this series we have discussed the electronic structure of the group IIIB dihydrides ScH_x, YH_x, and LuH_x as studied by optical spectroscopy[2] (paper I), self-consistent band calculations[3] (paper II), and photoelectron spectroscopy[4] (paper III). In a fifth paper, optical and photoemission techniques were used to examine the x-dependent properties of LaH_x, $1.9 \leq x \leq 2.89$, including the metal-to-semiconductor transition.[8] Our work has been complemented by recent band-structure calculations of Misemer and Harmon,[15] Switendick,[16–18] Gupta and Burger,[19–21] and Kulikov and co-workers.[22]

EXPERIMENTAL CONSIDERATIONS

Photoelectron spectroscopy is a versatile tool with which to probe the band-structure properties of a system. Measurements with polycrystalline samples such as hydrides (single crystals of dihy-

drides are not generally available) provide valuable information about features of the density of (occupied) states and, through studies of the $h\nu$ dependence of observed emission features, the angular momentum character of these states can be inferred.

The present measurements were performed using synchrotron radiation emitted by 240-MeV electrons stored in the Tantalus I electron storage ring. The radiation was dispersed with an ultrahigh vacuum 3m toroidal grating monochromator or a UHV 1m Seya-Namioka monochromator. The photon energy range was $7 \leq h\nu \leq 130$ eV; in this paper the low photon energy spectra are emphasized because the spectra change relatively little with $h\nu$ for $h\nu \gtrsim 40$ eV. All measurements were performed at 300 K in a UHV experimental chamber as discussed elsewhere[4,23] with operating pressure during measurements of $6-8 \times 10^{-11}$ Torr. Photoelectron energy analysis was done with a double-pass cylindrical mirror analyzer. The total resolution (electrons plus photons) ranged from 0.4 to 0.6 eV.

The samples used in this study were prepared in a separate hydrogen-charging system. In preparation for charging, posts of polycrystalline metal $\sim 2 \times 2 \times 10$ mm^3 were cut from crystal bar stock.[24] These posts were chemically polished (HF-HNO_3 solution), wrapped in Ta foil, then degassed *in situ* at 1000 °C before high-purity hydrogen was admitted to the charging vessel (pressure ~ 1 atm). The samples were then cooled and held at the temperature required to synthesize the desired hydride composition (575 °C for $TiH_{1.5}$, 600 °C for $HfH_{1.56}$, 600 °C for $ZrH_{1.87}$, 700 °C for $ZrH_{1.77}$, and 800 °C for $ZrH_{1.63}$). $ZrH_{1.94}$ was prepared by first charging at low pressure and subsequently exposing it to 150 atm of hydrogen at 600 °C. The hydrogen composition of sections taken from the samples studied was determined by hot vacuum extraction at 950 °C with an estimated accuracy of better than 1%.

Optical metallography showed the samples to be single phase. For ZrH_x, large columnar grains grew inward from the outer edges. X-ray analyses gave the following for ZrH_x: for $x = 1.63$, $a_0 = 4.781$ Å (fcc); for $x = 1.77$, $a_0 = 4.943$ Å and $c_0 = 4.493$ Å (fct); for $x = 1.86$, $a_0 = 4.965$ Å and $c_0 = 4.464$ Å (fct); for $x = 1.94$, $a_0 = 4.976$ Å and $c_0 = 4.454$ Å (fct). The volume of the ZrH_x unit cell increased from 109.3 Å^3 ($x = 1.63$) to 110.3 Å^3 ($x = 1.94$), an increase of 0.91%. In the fct phase, a_0 increased by 0.67% and c_0 decreased by 0.88% with $c/a = 0.909$ for $x = 1.77$ and $c/a = 0.895$ for $x = 1.94$. The large-grained ZrH_x samples were relatively rugged, the small-grained TiH_x samples were more brittle, and high-composition samples of HfH_x were extremely fragile.

The hydride samples were attached to copper holders and mounted on a sample bank (capacity ≈ 20) for photoemission measurements. Following a routine bake ($\lesssim 24$ h, $\lesssim 150$ °C), the operating vacuum of the measurement chamber was $\sim 6 \times 10^{-11}$ Torr. Immediately before study, the desired sample was retrieved from the bank with an x-y-z-θ-ϕ-tilt manipulator, fractured, and translated to the mutual focus of the monochromatic radiation beam and the electron energy analyzer. Data collection began within 2–3 min of sample fracture.

RESULTS AND DISCUSSION

fcc dihydrides

The photoelectron energy distribution curves (EDC's) for $TiH_{1.50}$, $ZrH_{1.63}$, and $HfH_{1.56}$ shown in Fig. 1 for $40 \leq h\nu \leq 80$ eV offer an overview of the electronic structure of these metal dihydrides. Two spectra for $TiH_{1.50}$ at $h\nu = 45$ and 80 eV show the metal d-derived emission band within ~ 3 eV of E_F and the covalent bonding band centered at about -5.5 eV extending from -3 to -10 eV. (All energies are referenced to the Fermi level E_F.) Energy distribution curves for $ZrH_{1.63}$ and $HfH_{1.56}$ reveal analogous band-structure features within ~ 10 eV of E_F. These band-structure features reflect the chemical bonding of the metal-hydrogen system. Also shown in Fig. 1 are the Ti 3p core levels (binding energy 33.3 eV), the Zr 4p's (28.1 and 29.5 eV), the Hf 5p's (30.3 and 38.3 eV), and the Hf 4f's (14.7 and 16.4 eV). Comparison of these binding energies with available literature values[25,26] for elemental Ti, Zr, and Hf shows the latter to be smaller by ~ 1 eV, consistent with charge redistribution away from the metal upon hydriding.[25] For $TiH_{1.5}$, the Auger structures centered at -16 eV (full width ~ 12 eV) result from the Auger decay of the Ti 3p core hole. For TiH_x with $33.3 < h\nu \lesssim 43$ eV, Auger and band-structure emission features overlap and the latter are obscured. Analogous Auger emission is shown for $ZrH_{1.63}$ at -17 eV for $h\nu = 40$ eV. For $HfH_{1.5}$ at $h\nu = 50$ eV, the Auger emission falls just below the $4f_{5/2}$ core level.

The experimental spectra of Fig. 1 indicate that the states contributing to the bonding bands of these dihydrides (as with others studied) are strongly hybridized, containing d as well as sp character. Were it not for this d character, the bonding band-emission features would diminish in strength with $h\nu$ as the photoionization cross section decreases. Furthermore, the double-structured Auger emission indicates two valence bands, each having d character, contributing to the decay of the np core hole.[4]

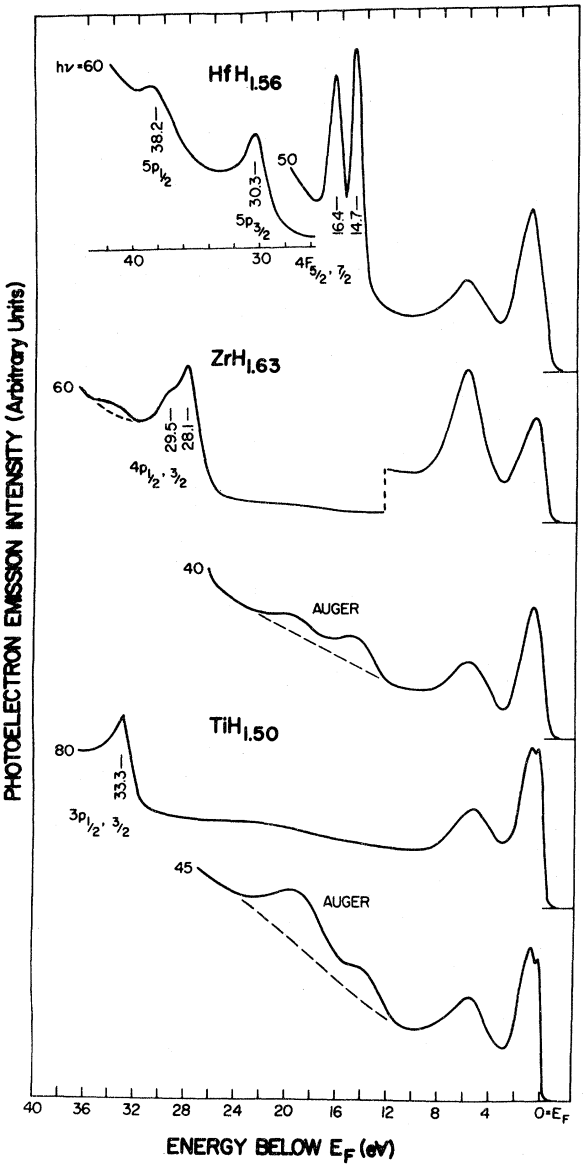

FIG. 1. Representative photoelectron energy distribution curves for $TiH_{1.50}$, $ZrH_{1.63}$, and $HfH_{1.56}$ showing the metal d-derived bands within ~3 eV of E_F, the hydrogen-induced bonding bands ~3–10 eV below E_F, and the core level emission for the Ti $3p$, Zr $4p$, Hf $5p$, and Hf $4f$ cores. The features labeled Auger arise from the Auger decay of the p-core hole; the double structural Auger emission reveals the d character of the bonding bands.

There have been three non-self-consistent calculations[16,19,22] of the band structure of TiH_2. In Fig. 2 the calculated bands of Gupta[19] for TiH_2 are reproduced. As shown, the Fermi level lies just above the L_3 and $\Gamma_{25'}$ symmetry points. The bands centered at – 6 eV constitute what we have termed collectively the "bonding band" (derived from hydrogen bonding and antibonding states). The bands near E_F are largely d derived, as can be seen, for example, by examining the calculations by Switendick[17] for the YH_0-YH_1-YH_2-YH_3 series.

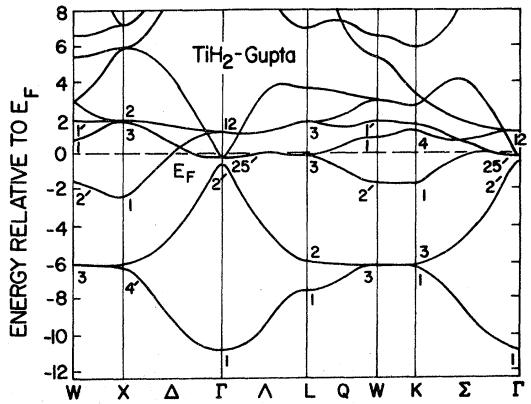

FIG. 2. Energy bands of TiH_2 calculated by Gupta (Ref. 19) showing the Fermi-level cutting band three between Γ and L. The tetragonal distortion lifts the degeneracy of $\Gamma_{25'}$ – Λ_3 – L_3 with one portion falling below E_F and the other above E_F (Jahn-Teller splitting). The bands within ~2 eV of E_F are largely d-like; the two bands centered at –6 eV give rise to the experimental features which we have termed the bonding or hydrogen-induced band.

The total density of states for TiH_2 is shown in the lower portion of Fig. 3 (dashed curve labeled TiH_2 DOS). From these calculations, a sharp peak is predicted at – 6 eV which is related to the flat bands near and along L-Q-W-K-X in the Brillouin zone.[3,4] The shoulder in the DOS at – 7.3 eV reflects the L_1 critical point.[3,4] Near E_F the calculations indicate a very high DOS peaking within a fraction of an electron volt of E_F originating from the flat band along Γ-Λ-L. The flat portion of the band extending from $W_{2'}$ to K_1 gives rise to the shoulder in the DOS at about – 2 eV.

The energy bands shown in Fig. 2 and the DOS of Fig. 3 are typical of the various calculations for dihydrides. These calculations predict a double-featured valence band made up of d-derived states near E_F and hybridized spd states ~6 eV below E_F.

Comparison of theory with the experimental results can be made through Fig. 3, where energy distribution curves for $TiH_{1.5}$, $ZrH_{1.63}$, $ZrH_{1.94}$, and $HfH_{1.56}$ taken at $h\nu = 21$ eV are reproduced. A smoothly varying background arising from scattered secondary electrons has been subtracted. The similarities for Ti, Zr, and Hf dihydrides are evident: All have structured emission within 3–3.3 eV of E_F and a deeper, structured, bonding band extending from –3 to –10 eV peaking at –5.1 to –5.5 eV with a shoulder near – 7.3 eV. For $HfH_{1.56}$ a

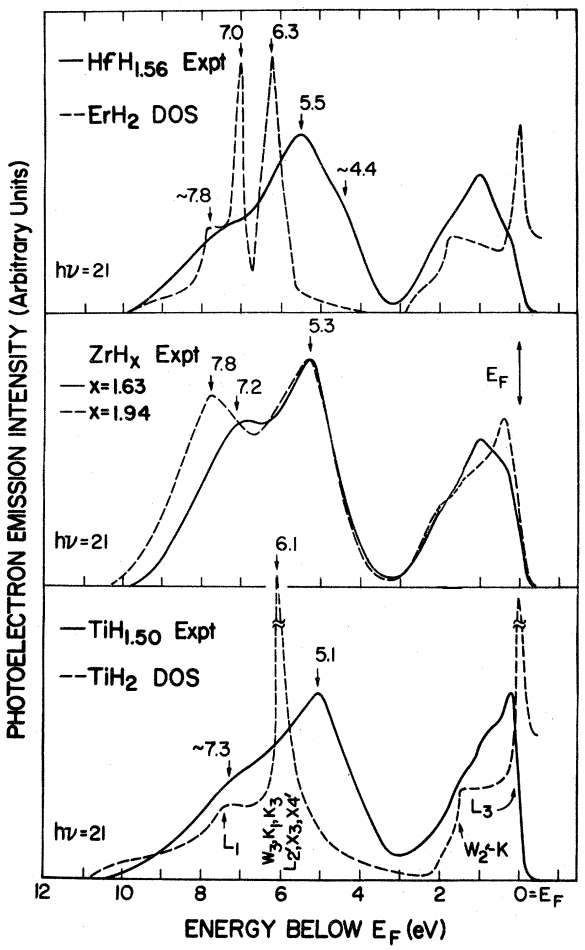

FIG. 3. Comparison of the calculated density of states for TiH_2 with our experimental photoelectron energy distribution curve for $h\nu = 21$ eV where the secondary electron background has been subtracted. Experiment shows the calculated bonding band to be too far from E_F with too small a full width at half maximum. The spectra for ZrH_x, $x = 1.63$ and $x = 1.94$, reveal the change in the band structure associated with the fcc→fct distortion, notably near E_F and near −7 eV. The experimental results for $HfH_{1.56}$ are compared to a rigid-band-shifted density of states of ErH_2 showing the theoretical basis for the 4-eV structure (greater dispersion in the bonding band compared to TiH_2). The experimental resolution was ~0.4 eV.

second shoulder appears at approximately − 4.4 eV. For each, the dominant central peak is associated with the predicted DOS structure and the deepest shoulder reflects the L_1 critical point.

Gupta's non-self-consistent calculations[19] for TiH_2 place the bonding-band center too far from E_F and its width is underestimated. Our own non-self-consistent calculations for YH_2 (Refs. 3 and 5) showed better agreement with the experimental bonding-band features. Our self-consistent prescription (including an improved method for handling exchange) led to bonding bands which were shifted ~1 eV toward E_F, so that iterating to self-consistency sacrificed agreement in those bands while improving agreement within the d bands near E_F.

While the TiH_2 calculations appear to underestimate the width of the d bands near E_F, they offer an explanation for the two features observed near − 1 and − 1.5 eV for TiH_2. We associate these features with the flat portion of the band along W-K and with the states near X.

For ZrH_2 and HfH_2 there have been no published band calculations. However, we can infer from Gupta's results (including those shown in Fig. 3), our own, those of Switendick, and those of Kulikov *et al.* that the dihydride bands and DOS will resemble those shown for TiH_2. To estimate differences, we reproduce in Fig. 3 the DOS calculated by Gupta[20] for ErH_2, where we have rigidly shifted E_F to account for the added electron in HfH_2 relative to ErH_2 (knowing this to be only a rough approximation). We schematically indicate that for ErH_2 (or HfH_2) the greater dispersion in the bonding bands (compared to TiH_2) results in more structure in the DOS. Experimentally we see that the photoemission density-of-states features for all three of these dihydrides are very similar. For $HfH_{1.56}$, an additional structure near − 4.4 eV is observed, consistent with the predictions for ErH_2. In Fig. 4, spectra at $h\nu = 15$ eV are shown

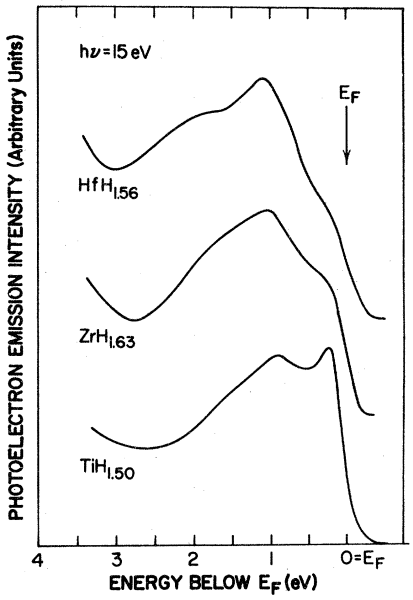

FIG. 4. Photoelectron emission spectra for fcc $TiH_{1.50}$, $ZrH_{1.63}$, and $HfH_{1.56}$ for $h\nu = 15$ eV emphasizing the d-band region near E_F. For $TiH_x \rightarrow ZrH_x \rightarrow HfH_x$ the width of the d band increases and the band along W_2-K_1 falls away from E_F.

for each of the cubic dihydrides for the d-band region. $TiH_{1.5}$ exhibits shoulders at -0.9 eV and -1.5 eV and a peak near E_F; $ZrH_{1.63}$ has a shoulder near -1.8 eV, a peak near -1.0 eV, and diminished Fermi-level emission. These features near -1 and -2 eV must be associated with the states along W-K and near X.

Comparison of experimental and calculational trends relating to the d bands indicates good qualitative agreement. The calculated width of the occupied d bands (i.e., $X_1 - E_F$) is smallest for ScH_2 (~ 1.9 eV) and increases to 2.4 eV for TiH_2 and 2.3 eV for YH_2. Experimentally, we have observed that the width of the occupied d bands increases in going across the Periodic Table (group IIIB to group IVB) or down the Periodic Table (3d to 4d transition-metal dihydrides).

fcc-fct distortion

Switendick,[16] Gupta,[19] and Kulikov *et al.*[22] have performed calculations which show that the doubly degenerate L_1 and the triply degenerate $\Gamma_{25'}$ states of TiH_2 lie just below the Fermi level and that the band along $\Gamma_{25'}$-Λ-L_3 crosses E_F twice. Earlier workers had observed an fcc-fct distortion of TiH_x and related it to a Jahn-Teller effect,[13,14] and the band-structure calculations supported that interpretation. According to the model proposed by Switendick, the Fermi level of fct TiH_x falls as hydrogen is removed until the occupied L_3 state is reached. When both of the L_3 states are empty, no total energy lowering can take place by splitting (distorting) and fct TiH_x is no longer energetically favored over fcc TiH_x.

This fcc-fct distortion of the group IVB dihydrides stands in contrast to the occupation of octahedral sites in the IIIB dihydrides prior to complete filling of all tetrahedral sites.[1,2,8-12,18] Apparently, in both cases the purely CaF_2 fcc energy states are energetically unfavorable for dihydrides with $x \simeq 2$. For group IIIB dihydrides, the total energy is lowered by occupation of the octahedral sites (the tendency to do so varies with the lattice constant) and in group IVB dihydrides the lattice distorts.

To reveal the x dependences of the electronic properties associated with the fcc-fct distortion, we have examined ZrH_x for $1.63 \leq x \leq 1.94$. The photoemission results are shown in Figs. 5 and 6 and in Fig. 3.

In Fig. 5 we show a series of EDC's for $ZrH_{1.63}$ (fcc) and $ZrH_{1.94}$ (fct) measured at room temperature. The vertical scales have been normalized for convenience to keep constant the height of the d-band emission maximum. The emission features for $ZrH_{1.94}$ are shown on the left; on the right we reproduce only the d bands for $ZrH_{1.63}$. Clearly, emission of states close to E_F is considerably more pronounced in $ZrH_{1.94}$ than in $ZrH_{1.63}$. The series of spectra for $h\nu = 14$ eV shown in Fig. 6 reveal the x dependence of the bands within 1.5 eV of E_F. For $x = 1.63$ (fcc), features are observed at -1.0 and -1.8 eV and the DOS appears to be diminishing as E_F is approached from below E_F. For $x = 1.75$ (fct) the Fermi-level emission is slightly enhanced (our instrumental resolution is $\simeq 0.4$ eV) and the lower two features appear unchanged. For $x = 1.88$, two distinct features appear at 1.25 and 1.9 eV and the Fermi-level emission is much more prominent. For $x = 1.94$, the Fermi-level emission is much greater than that of the features near 1.25 and 1.9 eV and the latter appear to have shifted or broadened almost beyond recognition. We associate these changes with the predicted splitting of the degenerate L_3-Λ_3-Γ'_{25} states, a splitting which increases as the distortion increases (i.e., with increasing hydrogen content). As shown, a change in hydrogen concentration of $\sim 10\%$ results in a major band-structure modification near E_F. (Note that in Switendick's calculation for fct TiH_x with $c/a = 0.972$ the calculated L_3 splitting was ~ 0.2 eV; for ZrH_x with $c/a \simeq 0.9$ we see experimentally that the distortion is much greater.)

In the emission spectra for $ZrH_{1.94}$ ($14 \leq h\nu \leq 26$ eV) shown in Fig. 5, two features appear in the bonding band, namely, the peak at -5.3 eV, which is nearly invariant with $h\nu$, and the deeper shoulder near -7 eV which disperses with $h\nu$. The $h\nu$ dependence of the -7 eV peak energy is shown in the inset of Fig. 5; it moves downward ~ 1 eV for $h\nu$ increasing from 15 to 26 eV. At higher photon energy it is obscured by overlapping Auger emission and ultimately it is lost because of its low angular momentum character. This feature reflects the L_1 band, as discussed in detail in III and supported by the calculations and l projections of II.

In the inset of Fig. 5, results for samples of three different compositions are shown, namely, $x = 1.63$, 1.75, and 1.94. With increasing x, the shoulder moves to higher binding energy compared to the same feature observed at the same photon energy for a lower-x dihydride. This indicates a lowering in energy of the L_1 critical point caused by the tetragonal distortion. That shift amounts to ~ 0.65 eV for $ZrH_{1.63}$ (cubic) $\rightarrow$ $ZrH_{1.94}$ (fct with $c/a = 0.909$).

In Fig. 3, spectra for $ZrH_{1.63}$ and $ZrH_{1.94}$ are shown for $h\nu = 21$ eV free of the secondary background. There, the change in the -7 eV feature is clearly evident: It is a shoulder at -7.2 eV for the cubic phase and it is a well defined maximum

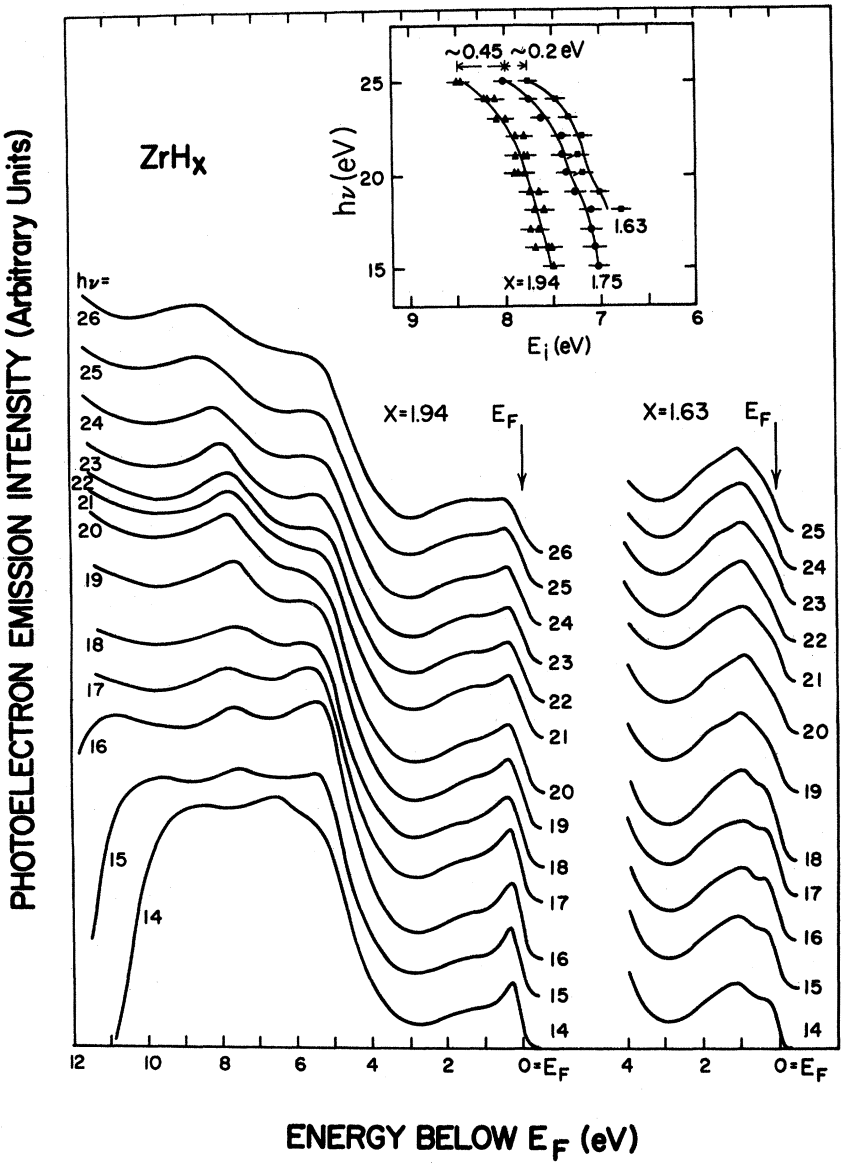

FIG. 5. Photoelectron energy distribution curves for fcc $ZrH_{1.63}$ and fct $ZrH_{1.94}$. For $x=1.63$, features are observed at -1 and -1.8 eV and are larger at all $h\nu$ than the emission just below the Fermi-level cutoff. For $x=1.94$, the Fermi-level emission is dominant and the deeper features in the d bands are less pronounced. Within the bonding band, the shoulder at ~7 eV shows the same $h\nu$ dependence (inset) for different values of x but falls farther from E_F with increasing x. No change in the feature at ~5.3 eV is observed as a function of x. No such change has been observed as a function of x for YH_x, which does not exhibit the fct distortion.

at – 7.8 eV for the tetragonal phase. At the same time the central peak at – 5.3 eV is nearly independent of x.

CONCLUSIONS

The group IV*B* dihydrides display d-derived emission features within ~3 eV of E_F which can be associated with the band along $W_{2'}-K_1$. The bonding bands extend from – 3 to – 10 eV and are centered at approximately – 5.5 eV. Experimentally, the width of the d bands has been shown to follow the calculational trends by increasing in going from group III*B* to group IV*B* dihydrides. The center of the bonding band is observed at approximately the same energy for all dihydrides, leading us to conclude that stable dihydrides favor a bonding band centered near – 5.5 eV. Photoemission results bridging the fcc-fct distortion in ZrH_x are consistent with a Jahn-Teller splitting

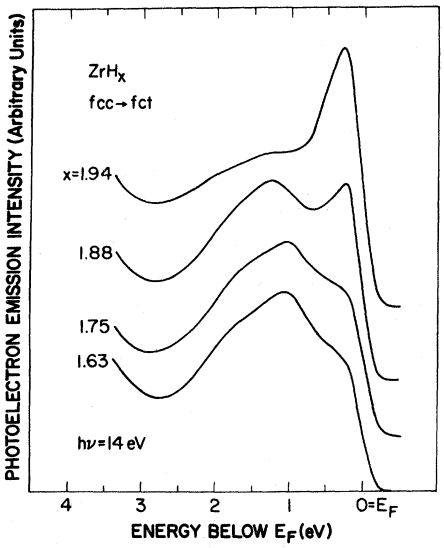

FIG. 6. Photoemission spectra showing the x dependence of the d-band spectrum. With increasing x, the fct distortion increases and the Fermi-level emission becomes successively more dominant as the bands along Γ-Λ-L split apart.

of the bands near E_F, showing a change in Fermi-level emission with increasing x. In contrast to this, x dependences of photoemission spectra for cubic YH_x, $1.7<x<1.98$ are very slight and reflect octahedral site occupancy.[2,4] Also associated with the tetragonal distortion is a shift to greater binding energy of the critical point at L_1.

ACKNOWLEDGMENTS

We have profited from discussions with A. C. Switendick and B. N. Harmon. We are grateful to H. H. Baker and A. D. Johnson for expert assistance in preparation and characterization of the samples and for the amiable cooperation of the staff of the SRC. The work at the University of Wisconsin was supported by the NSF through the International Programs Division under Grant No. INT80-01673; The Ames Laboratory is operated for the U. S. Department of Energy by Iowa State University under Contract No. W-7405-Eng-32 and is supported by the Office of Basic Energy Sciences Contract No. WPAS-KC-02-01. The SRC is supported under Contract No. NSF DMR 78-21888.

[1]*Metal Hydrides*, edited by W. M. Mueller, J. P. Blackledge, and G. G. Libowitz (Academic, New York, 1968).
[2]J. H. Weaver, R. Rosei, and D. T. Peterson, Phys. Rev. B 19, 4855 (1979) (referred to in text as paper I). A review of many of the points made in Refs. 2-8 can be found in J. H. Weaver and D. T. Peterson, J. Less-Common Met. 74, 207 (1980).
[3]D. J. Peterman, B. N. Harmon, J. Marchiando, and J. H. Weaver, Phys. Rev. B 19, 4867 (1979) (referred to in text as II).
[4]J. H. Weaver, D. T. Peterson, and R. L. Benbow, Phys. Rev. B 20, 5301 (1979) (referred to in text as III).
[5]D. J. Peterman and B. N. Harmon, Phys. Rev. B 20, 5313 (1979) (companion paper to Ref. 4).
[6]J. H. Weaver, R. Rosei, and D. T. Peterson, Solid State Commun. 25, 201 (1979).
[7]J. H. Weaver, J. A. Knapp, D. E. Eastman, D. T. Peterson, and C. B. Satterthwaite, Phys. Rev. Lett. 39, 639 (1977).
[8]D. J. Peterman, J. H. Weaver, and D. T. Peterson, Phys. Rev. B (in press).
[9]D. S. Schreiber and R. M. Cotts, Phys. Rev. 131, 1118 (1963).
[10]E. L. Venturini and P. M. Richards, Solid State Commun. 32, 1185 (1979) and E. L. Venturini, J. Appl. Phys. 50, 2053 (1979).
[11]D. Khatamian, W. A. Kamitakahara, R. G. Barnes, and D. T. Peterson, Phys. Rev. B 21, 2625 (1980).
[12]D. L. Anderson, R. G. Barnes, D. T. Peterson, and D. R. Torgeson, Phys. Rev. B 21, 2625 (1980).
[13]F. Ducastelle, R. Candron, and P. Costa, J. Phys. (Paris) 31, 57 (1970).
[14]H. Nagel and H. Goretzki, J. Phys. Chem. Solids 36, 431 (1975); H. Nagel and R S. Perkins, Z. Metallkd. 66, 362 (1975).
[15]D. Misemer and B. N. Harmon (unpublished).
[16]A. C. Switendick, J. Less-Common Met. 49, 283 (1976); see also A. C. Switendick, in *Hydrogen in Metals I: Basic Properties*, Vol. 28 of *Topics in Applied Physics*, edited by G. Alefeld and J. Volkl (Springer, Berlin, 1978), p. 101.
[17]A. C. Switendick, Solid State Commun. 8, 1463 (1970).
[18]A. C. Switendick, J. Less-Common Met. (in press).
[19]M. Gupta, Solid State Commun. 29, 47 (1979).
[20]M. Gupta, Solid State Commun. 27, 1355 (1978).
[21]M. Gupta and J. P. Burger, Phys. Rev. B 22, 6074 (1980).
[22]N. I. Kulikov, V. N. Borzunov, and A. D. Zvonkov, Phys. Status Solidi B 86, 83 (1978).
[23]G. Margaritondo, J. H. Weaver, and N. G. Stoffel, J. Phys. E 12, 662 (1979).
[24]Impurity analysis of crystal-bar Zr and Hf and selected-quality commercial Ti in parts per million by weight for impurities in (Ti, Zr, Hf) is as follows: Al (1,30,40), Cu (10,0.5,40), Cr (30,30, <10), Fe (90,200,100), Mn (20, <10, <10), Mg (10, <10, <10), Ni (20,30, <10), Si (30,20, –), N (20,30,20), O (200, 200,500), C (100 in Zr), Hf (40 in Zr).
[25]B. W. Veal, D. J. Lam, and D. G. Westlake, Phys. Rev. B 19, 2856 (1979).
[26]P. Steiner, H. Hochst, J. Schneider, S. Hüfner, and C. Politis, Z. Phys. B 33, 241 (1979).